Vol. 13, No. 1 (2025), pp.105–118

CHITKARA UNIVERSITY

Journal of Pharmaceutical Technology Research and Management

Formulation, Optimization, and Characterization of Hepatoprotective Polyherbal Tablet

Kamaljeet[1], Rameshwar Das[1], Priyanka Kriplani[1] and Prabhjot Kaur[1]*

[1]*Department of Pharmaceutical Science, Guru Gobind Singh College of Pharmacy, Yamunanagar, Haryana, India.*

*prabhjotkaur102001@gmail.com (Corresponding Author)

RESEARCH ARTICLE **Open Access**

ARTICLE INFORMATION

Received: October 31, 2025
Accepted: November 20, 2025
Published Online: December 20, 2025

Keywords:
Liver cirrhosis, Hepatoprotective, Tablet, Herbs, Phytochemicals, Controlled release

DOI: 10.15415/jptrm.2025.131008

ABSTRACT

Background: Liver cirrhosis is a liver disease with a high mortality rate worldwide, and antifibrotic drugs are generally used for alleviating symptoms, but there are still limitations of current therapies. Research is going on new therapies including herbals for management of cirrhosis.

Objective: Literature-based research identifies curcumin, hesperidin, Aegle marmelos (bael), Solanum nigrum (black nightshade), and Silybum marianum (milk thistle) as hepatoprotective phytoconstituents and herbs. The current study aims to develop and evaluate a hepatoprotective polyherbal tablet.

Methods: Tablets were prepared using the direct compression method utilizing polymers including microcrystalline cellulose, starch, etc. Response surface methodology (central composite design) was used for optimizing formulation, taking hardness and disintegration time as dependent variables. The prepared formulations were characterized using parameters including weight variation, friability, thickness, percentage drug release, etc. Furthermore, formulations were evaluated for release kinetics studies.

Results: Optimized formulation (F14) revealed percentage drug release from 71.57–94.91%. Furthermore, other parameters were also found to be satisfactory. Results from kinetics study revealed that F14 followed the Hinton-Crowell model with non-fickian release mechanism.

Conclusion: Polyherbal hepatoprotective tablets can be used for sustained delivery of polyherbs as an alternative therapy for management of liver cirrhosis and hepatoprotective action. Furthermore, pre-clinical and clinical studies should be done for better applicability.

1. Introduction

Liver is considered one of the essential organs that weighs about 1.4 kg in humans. It is necessary for the metabolism, synthesis, storage, and detoxification of both endogenous and foreign chemicals. It also facilitates the production of hormones and serum proteins, the elimination of both naturally occurring and exogenous chemicals, the metabolism of fats and carbohydrates, and other functions. The liver is very susceptible to disease and can potentially be lethal because of its many functions (Devarbhavi *et al.*, 2023). An intricate organ essential to life is the liver. Liver diseases are a major global public health concern that jeopardize the health of billions of people (Terrault *et al.*, 2023). The four primary forms of liver disease are cirrhosis, fatty liver, liver cancer, and hepatitis. Furthermore, hepatitis and liver cancer rank among the most significant worldwide public health concerns, according to (Devarbhavi *et al.*, 2023; Terrault *et al.*, 2023).

Cirrhosis is a significant cost on a global scale. According to a study, alcohol-related liver cirrhosis declined from 80% to 58%, but prevalence of unspecified cirrhosis will outnumber alcohol-related cirrhosis from 2027 (Kornerup *et al.*, 2025). Finding therapy options for common liver illnesses is difficult. Colchicine, Ursodiol, antibiotics, corticosteroids, interferon, penicillamine, and antiviral medicines are among the most effective treatments that are incompatible, but the rate of side effects is high (Mancak *et al.*, 2024). Alternative medications that are less harmful and more effective must be developed for treating hepatic disorders. Primarily, almost 80% of people on this planet have used plant-based medicines as traditional forms of treatment. Numerous medicinal plants and their preparations have been shown to have hepatoprotective properties all around the world. Nearly 160 chemical components from 101 plants have been shown to have liver-protective qualities (Park *et al.*, 2022).

One of the main ingredients that is present in large quantities in citrus fruits is hesperidin (HSP). An antioxidant called hesperidin may help shield the body from harm caused by free radicals. Hesperidin administration restored membrane function by keeping liver enzyme levels close to normal and is being researched in treating numerous fatty liver diseases (Cofano *et al.*, 2025; Li *et al.*, 2022; Morshedzadeh *et al.*, 2023; Sivaslioglu *et al.*, 2024; Yari *et al.*, 2021). Curcumin (Curcuma longa Linn., Zingiberaceae family) is a yellow colour pigment found in rhizome of turmeric. The pharmacological effects of curcumin include anti-oxidant, anti-inflammatory as well as anti-oncogenic properties. Curcumin significantly reduces liver cirrhosis by acting on many routes, according to recent research (Mirhafez *et al.*, 2021; Ngu *et al.*, 2022; Różański *et al.*, 2021; Shahrebabak *et al.*, 2025). Additionally, Aegle marmelos (Bael), a small to medium-sized tree or deciduous shrub that belongs to the Rutaceae family, has hepatoprotective properties (Bhardwaj *et al.*, 2015; Singanan *et al.*, 2007). S. nigrum is a herb that is a member of the Dicotyledonae class and the Solanaceae family. In addition to its hepatoprotective properties, S. nigrum is often referred to as black nightshade, garden nightshade, or blackberry nightshade. Being naturally occurring antioxidants, anthocyanins can stop the oxidative stress brought on by acute liver toxicity. One of the best sources of phenolic compounds, such as gallic acid, quercetin, and others, is S. nigrum. These compounds work as an active ingredient in regulating oxidation, preventing oxidative stress, acute liver toxicity, metabolic diseases like diabetes, and various cancers (Khonche *et al.*, 2019; Tang *et al.*, 2022; Tiwari *et al.*, 2022). Furthermore, it has been demonstrated that *Silybum marianum* L. (S. marianum) was used in the Western world to treat liver and gallbladder problems as early as the fourth century BC. Furthermore, it has been demonstrated to exhibit anti-oxidant, immunomodulatory, liver-regenerating, inflammatory, and anti-fibrotic properties in patients with viral hepatitis, drug-induced liver injury, non-alcoholic fatty liver disease, and fatty liver disease (Shaker *et al.*, 2010). According to research, silymarin has pharmacological effects that include neuroprotection, lowering blood lipids, reducing inflammation, immunological modulation, and preventing diabetes. It also suppresses several forms of cancers. Furthermore, silymarin has a number of pharmacological properties that can help with liver detoxification, liver cell membrane protection, liver cell degradation prevention, and liver purification (Aghazadeh *et al.*, 2011; Federico *et al.*, 2017; Jiang *et al.*, 2022; Vlizlo *et al.*, 2023). Tablets are among the most widely used and adaptable types of medication dosage. The oral route of administration is the most popular approach for systemic effects due to its ease of use, pain avoidance, variety, and most importantly patient compliance (Zhang *et al.*, 2023). Developing and testing a poly-herbal tablet formulation for hepatoprotective effect is the aim of this work.

2. Material and Methods

2.1. Chemicals

Hesperidine as well as curcumin were procured from Chemika-Biochemika Reagent and Sanat Products Limited, Delhi, respectively. Microcrystalline cellulose, starch, polyvinylpyrrolidone (PVP) K 30, sodium bicarbonate, and magnesium stearate were acquired from Titan Biotech Ltd. Bhiwadi, Rsearch-Lab Fine Chem Industries Mumbai, V.K Chemical Industries, Nice Chemicals (P) Ltd. Kerala, Qualikems Fine Chem Pvt Ltd. Vadodara, Nice Chemicals (P) Ltd. Kerala, and Qualikems Fine Chem Pvt Ltd. Vadodara, respectively. Solvents including ethanol and methanol were procured from Changshu Hongsheng Fine Chemical Co. Ltd., Changshu City.

2.2. Preparation of Extract

- **Aegle Marmelos** The gathered leaves were cleaned and allowed to air dry before being stored in tightly sealed containers as powder. Using a Soxhlet device, leaves (1 kg of each portion) were extracted with ethanol in a sequential manner using a hot extraction method. The produced extract was kept in a vacuum desiccator until it was needed again after the ethanol had dried off at 40°C (Gupta *et al.*, 2018).
- **Solanum Nigrum** The leaves were cleaned, chopped into tiny bits, and allowed to dry in the shade for three days. The 800 g of dried SN was moistened with water and then continuously heated (100°C, 40 min) using a Soxhlet device. After filtering, the resultant water extract was concentrated in a water bath at 90°C until it turned into a creamy paste and kept in the freezer until it was needed again (Solati *et al.*, 2014).
- **Silybum Marianum** 100 g of dry powdered *Silybum marianum* was extracted using 500 ml of 70% ethanol by utilizing Soxhlet apparatus. The resultant extract was then filtered, concentrated in a water bath at 90°C, and kept at –20°C until it was needed for more research (Lukic *et al.*, 2022).

2.3. Pre-formulation Study

In drug research and development programs, pre-formulation investigations (physicochemical and biopharmaceutical properties) are crucial because they provide valuable information on drug identification and optimization. Pre-formulation data provides guidance for clinical evaluation, formulation development, and bulk manufacturing processes (Robinson *et al.*, 2015).

- **Organoleptic Properties** The organoleptic properties such as colour, odour, and texture of the test samples were studied by visual inspection.
- **Fourier Transform Infrared Spectrum (FTIR)** To analyze the structures and compatibility of chemicals used in the manufacture of formulation, FTIR analysis was undertaken. The FTIR spectrophotometer (Bruker Corporation, Massachusetts) was used to analyze the FTIR spectra of the drugs and excipients after they had been entrained with potassium bromide (KBr) disc (Morteza-Semnani *et al*., 2022).
- **Differential Scanning Calorimetry (DSC) Analysis** The most popular thermal method used to check for excipients incompatibility is differential scanning calorimetry (DSC). This method typically yields findings really quickly and only needs a minimal sample size. According to the study's findings, DSC aids in identifying any incompatibilities between the formulation's constituent parts. These could be enthalpy curves, endothermic or exothermic peaks, or changes in appearance. DSC frequently entails subjecting the formulations to temperatures as high as 300°C, which can destroy excipients (Q10, TA Instruments Waters) (Morteza-Semnani *et al*., 2022).
- **Preparation of Calibration Curve**
    - **Curcumin** A 100 milliliter volumetric flask was filled with 10 milligrams of carefully weighed curcumin. Methanol was added until the target concentration of 100 µg/ml of stock solution was achieved. The stock solution yielded corresponding concentrations of 5–25 µg/ml. Using a UV spectrophotometer and a blank solvent, the curcumin solution was scanned in the 200–800 nm range. The wavelength corresponds to the maximum absorbance of curcumin in the solvent, which is 280 nm. After that, the curcumin calibration curve was shown, with absorbance on the y-axis and concentration on the x-axis (Majumder *et al*., 2022).
    - **Hesperidin** Ten milligrams of hesperidin were carefully weighed and transferred to a 100 milliliter volumetric flask to achieve a concentration of 100 µg/ml of stock solution. Then, a solvent mixture of methanol and water (1:1) was used to boost the volume to 100 ml. From the stock solution, concentrations of 15–30 µg/ml were now attained. The samples were scanned using the UV spectrum between 200 and 400 nm. Hesperidin showed the highest absorption at 284 nm (Chimagave *et al*., 2022). A graph demonstrating the absorbance (Y-axis) and concentration (X-axis) was shown.
    - **Aegle Marmelos Leaves Extract** After precisely weighing 25 mg of *Aegle marmelos* leaf extract, it was placed in a 50 ml volumetric flask. Then, ethanol was added to the flask in the proper volume to dissolve the 25 mg sample and bring the volume up to the 50 ml mark. Now pipette out 5 ml of the first dilution and pour it into a 50 ml volumetric flask. After that, the solvent should be added to the volume until the concentration is 50 µg/ml of stock solution. Pipette out 2 ml, 4 ml, 6 ml, and 8 ml of the stock solution into four different 10 ml volumetric flasks to get a concentration of 10–40 µg/ml. The samples were analyzed in the UV region of 200–400 nm. The maximum absorption was observed at 269 nm (Ahmad *et al*., 2021). The concentration (X-axis) and absorbance (Y-axis) were shown on a graph.
    - **Solanum Nigrum Leaves Extract** Weigh 25 mg of leaf extract from *Solanum nigrum* into a 50 ml volumetric flask, then add distilled water as a solvent to dissolve the sample and get the desired result. Pipette out 1 ml, 2 ml, 3 ml, 4 ml, and 5 ml from the initial dilution and move them to five different 10 ml volumetric flasks in order to reach a concentration of 50–250 µg/ml. The volume should then be adjusted to 10 ml. The samples were analyzed in the UV region of 200–400 nm. The maximum absorption was observed at 317 nm (Panchal *et al*., 2025). A graph displaying the absorbance (Y-axis) and concentration (X-axis) was displayed.
    - **Silybum Marianum Seed Extract** Fill a 50 ml volumetric flask with 25 mg of *Silybum marianum* seed extract. Then, add enough ethanol to the flask to dissolve the 25 mg sample and bring the volume up to the 50 ml mark. To achieve a concentration of 20–60 µg/ml, pipette out 2 ml, 3 ml, 4 ml, and 5 ml from the initial dilution and transfer them to five distinct 50 ml volumetric flasks. Then, added phosphate buffer pH 6.8 to bring the volume up to 50 ml. The samples were examined in the 200–400 nm UV range. At 275 nm, the highest absorption was recorded (Mukhtar *et al*., 2023). The *Silybum marianum* seed extract calibration curve was then plotted, with concentration on the x-axis and absorbance on the y-axis.

2.4. Pre-compression Evaluation

Hausner's ratio (HR), Carr's compressibility index, bulk density, tapped density, and angle of repose were all computed using established methods for the pre-compression study. Three duplicates of each determination were made.

- **Bulk density** A 25 ml measuring cylinder was filled with 10 g of the excipients mix after it had been weighed. The bulk volume was determined by measuring the volume.

$$\textbf{\textit{Bulk density}} = Weight\ of\ \ powder\ mix\,(g) \,/\, Bulk\ volume\ of\ \ powder\ mix \tag{1}$$

- **Tapped density** One hundred tappings of the excipients powder mixture in the 25 ml measuring cylinder were made, and the new volume was noted as the tapped volume.

$$\textbf{\textit{Tapped density}} = Weight\ of\ the\ powder\ mix\,(g) \,/\, Tapped\ volume\ of\ the\ powder\ mix \tag{2}$$

- **Carr's index** Carr's index indicates the compressibility or free-flowing property of powder. This was calculated using the formula:

$$\textbf{\textit{Carr's index}} = (Tapped\ density - Bulk\ density) \,/\, Tapped\ density \times 100\% \tag{3}$$

- **Hausner's ratio** Hausner's ratio indicates the cohesiveness of powder. This was calculated using the formula:

$$\textbf{\textit{Hausner's ratio}} = Tapped\ density \,/\, Bulk\ density \tag{4}$$

- **Angle of repose** The funnel approach was applied. To create a heap (cone) at the base, the excipients powder mixture was poured through a funnel that was clamped to a retort stand. The formula was used to determine the angle of repose (θ), which was the angle formed by the powder mix with the base.

$$\tan\theta = h / r \tag{5}$$

Where h = height of the heap (cone) and r = radius of the cone (Ravikkumar *et al.*, 2024).

2.5. Experimental Design

Utilizing Design Expert (version 13) software, polyherbal hepatoprotective tablets were developed and optimized utilizing central composite design (Narukulla *et al.*, 2024). Using two independent variables, namely (Factor-A) MCC (%) and (Factor-B) starch (%), thirteen distinct formulations (F1–F13) were created. As seen in Tables 1 and 2, starch (%) maintains PVP, magnesium stearate, and medications constant. Disintegration time (R2) and hardness (R1) were selected as dependent response variables.

Table 1: Actual and Coded Level of the Factor

Independent Variables	**Actual Values**		**Coded Level**	
	Low Value	High Value	Low Level	High Level
Factor A	50	60	-1	+1
Factor B	30	40	-1	+1
Response				
Dependent Variables	Hardness (R1)		Kg/cm^2	
	Disintegration Time (R2)		Second	

Table 2: Composition of Polyherbal Tablets

Ingredients (mg)	**F1**	**F2**	**F3**	**F4**	**F5**	**F6**	**F7**	**F8**	**F9**	**F10**	**F11**	**F12**	**F13**
MCC	50	55	55	50	60	55	55	47.93	55	62.07	60	55	55
Starch	40	27.93	35	30	30	35	35	35	35	35	40	35	42.07
Polyvinyl pyrrolidone K 30	06	06	06	06	06	06	06	06	06	06	06	06	06
Sodium bicarbonate	03	03	03	03	03	03	03	03	03	03	03	03	03
Magnesium stearate	01	01	01	01	01	01	01	01	01	01	01	01	01
Hesperidine	30	30	30	30	30	30	30	30	30	30	30	30	30

Ingredients (mg)	**F1**	**F2**	**F3**	**F4**	**F5**	**F6**	**F7**	**F8**	**F9**	**F10**	**F11**	**F12**	**F13**
Curcumin	30	30	30	30	30	30	30	30	30	30	30	30	30
Aegle marmelos leaves extract (mg)	30	30	30	30	30	30	30	30	30	30	30	30	30
Solanum nigrum leaves extract (mg)	30	30	30	30	30	30	30	30	30	30	30	30	30
Silybum marianum seed extract (mg)	30	30	30	30	30	30	30	30	30	30	30	30	30

2.6. Formulation of Tablets

The direct compression method was used to prepare the tablets. Every excipient was sieved using a 20-mesh screen. Using a mortar and pestle, these excipients were combined in the precise ratio specified in Table 4.7. Next, weigh the medicine according to the table and mix it with the excipients in a mortar and pestle for five minutes. A Stokes single-punch tableting machine was used to manufacture the tablets by direct compression (Tafere *et al.*, 2021).

2.7. Evaluations of Tablets

- **Weight Variation** Twenty pills were chosen at random from each batch to guarantee consistency in tablet weight, and the average weight was calculated. The weight of each tablet was then contrasted with the mean weight. In accordance with the established guidelines, the percentage deviation was computed and weight variation was verified (Ravikkumar *et al.*, 2024).
- **Hardness** To determine the hardness of a tablet, they used a Monsanto hardness tester. Tablet hardness was determined by taking the average value with standard deviation of three tablets from each batch. It is expressed in kg/cm².
- **Thickness and Diameter** A Vernier caliper was used to measure the thickness of ten randomly chosen tablets. Mean values ± SD were used to express the results (Ravikkumar *et al.*, 2024).
- **Friability** The Roche friabilator was used to evaluate the tablets' friability. After weighing ten tablets from each formulation batch, they were put in a Roche friabilator and rotated 100 times at 25 rpm for four minutes. The final weight was then determined (Tafere *et al.*, 2021). The following calculation was used to determine the percentage of friable loss:
- **Disintegration Time** Six polyherbal tablets were chosen at random from each formulation in order to calculate the disintegration time. The disintegration medium was water, and the temperature was kept at 37 ± 0.5 °C. For computation, the average disintegration time of six tablets was recorded (Ravikkumar *et al.*, 2024).
- **Drug Content Uniformity** To ensure uniform drug distribution, ten tablets were triturated to a fine powder. A UV-Visible Spectrophotometer was used to measure absorbance after the powder containing 10 mg of the medication was weighed and dissolved in 100 cc of phosphate buffer with a pH of 6.8. The amount of medication was determined using the standard calibration curve's slope (Sharma *et al.*, 2023).
- **In Vitro Drug Release** The in vitro drug release studies were carried out for one hour in 900 milliliters of phosphate buffer pH 6.8 as the dissolving medium using a paddle-style dissolution test apparatus. The temperature was maintained at 37 ± 0.5 °C, and the paddle was set at 100 rpm for the duration of the experiment. A 5 ml sample was extracted at several times during the hour. Each sample was filtered through a membrane filter with a pore size of 0.45 mm after being properly diluted, and it was then analyzed using a UV spectrophotometer (Musuc *et al.*, 2021).
- **Release Kinetics Studies** Numerous kinetic models, such as the zero-order release model, first-order release model, Higuchi model, Hixson–Crowell cube root law, and Korsmeyer–Peppas model, were employed to assess the in vitro release data and characterize the release kinetics (Zhao *et al.*, 2021).

3. Results and Discussions

3.1. Extraction Yield

The percentage yields of Soxhlet extractions utilizing three medicinal plants with different solvents are displayed in Table 3.

Table 3: Percentage Yield of Extracts Used in the Study

Plant Name	**Part Used**	**Solvent**	**Percentage Yield (% w/w)**
Aegle marmelos	Leaves	Methanol	4.21
Solanum nigrum	Leaves	Aqueous	5.09
Silybum marianum	Seed	Ethanol	1.84

3.2. Pre-formulation Studies

- **Organoleptic Properties** The organoleptic properties used to describe their colour, odour, and physical form are listed in Table 4.

Table 4: Organoleptic Properties of Phytochemicals as Well as Extracts Used in the Study

Phytochemical/ Extract	Color	Odour	Physical Form
Hesperidin	Pale yellow	Characteristic	Powder
Curcumin	White	Characteristic	Powder
Aegle marmelos extract	Dark green	Characteristic	Semi-solid
Solanum nigrum extract	Dark brown	Characteristic	Semi-solid
Silybum marianum extract	Brown	Characteristic	Semi-solid

- **FTIR Study**

The spectra of curcumin represent characteristic bands at 3425 cm^{-1} (O–H group); 2922 cm^{-1} (C–H stretching); 1032 cm^{-1} (C–O stretching); 1627 cm^{-1} (C=C stretching). O–H (phenolic) is indicated by the presence of a peak at 1184 cm^{-1}, and C–H vibration of the aromatic ring occurred at 814 cm^{-1} respectively. It is shown in Figure 1(a).

The spectra of hesperidin represent characteristic bands at 3426 cm^{-1} (O–H group); 2918 cm^{-1} aromatic (C–H stretching); 1277 cm^{-1} (C–O stretching); 1183 cm^{-1} (C–O stretching) respectively (Figure 1(b)).

The *Aegle marmelos* methanolic extract FTIR spectra show distinctive bands at 3381 cm^{-1} (O–H stretching), 2962 cm^{-1} (C–H stretching), and 1710 cm^{-1} (C=O stretching), which point to the existence of certain functional groups in the molecule, shown in Figure 1(c).

The presence of distinct functional groups within the compound is suggested by the distinctive bands found in the FTIR spectra of the *Solanum nigrum* aqueous extract at 3390 cm^{-1} (N–H stretching), 2962 cm^{-1} (C–H stretching), and 1316 cm^{-1} (C=O stretching) respectively, shown in Figure 1(d).

Furthermore, it is evident from the *Silybum marianum* ethanolic extract's FTIR spectra that the compound contains unique functional groups at 3412 cm^{-1} (O–H stretching), 2925 cm^{-1} (C–H stretching), 2824 cm^{-1} (=C–H), and 1742 cm^{-1} (C=O stretching), as shown in Figure 1(e).

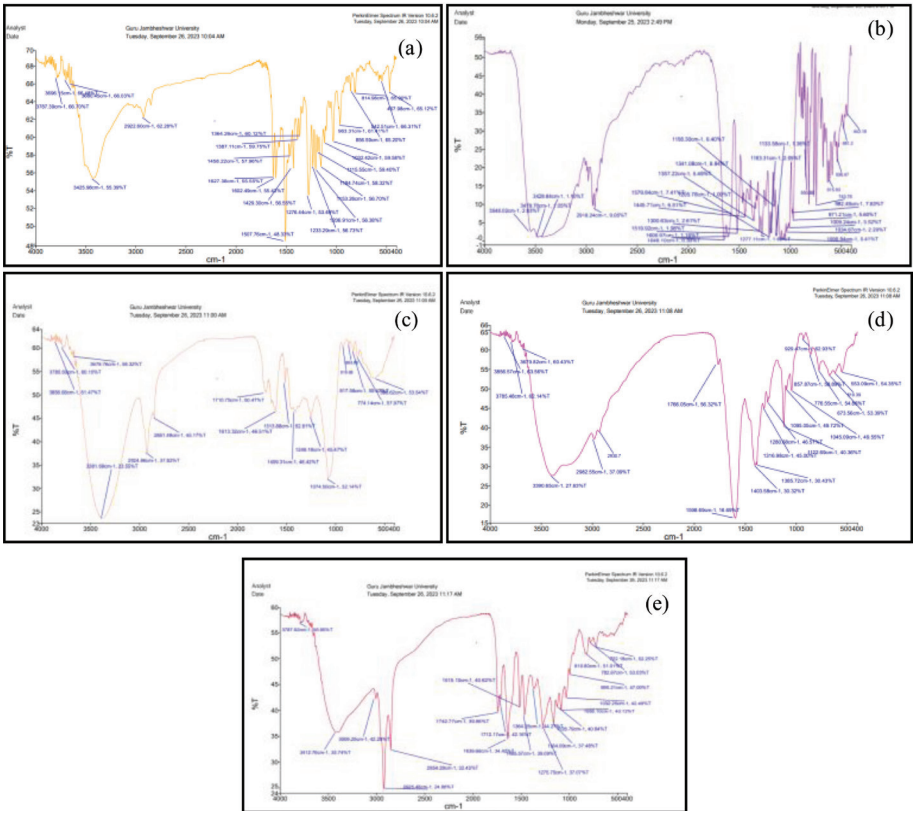

Figure 1. FTIR spectrum for (a) curcumin, (b) hesperdin, (c) *Aegle marmelos* extract, (d) *Solanum nigrum* extract, and (e) *Silybum marainum* extract.

- **Differential Scanning Colorimetry (DSC) Study**

Endothermic peak of DSC indicates melting point of curcumin is 180.04 □ as per the melting point within the range 179–182 □ by the reference standard drug (Figure 2 (a)). The endothermic peak of DSC for hesperidin (Figure 2 (b)) was within the limit (258–262 □). Furthermore, Aegle marmelos methanolic extract (Figure 2 (c)), Solanum nigrum extract (Figure 2 (d)), and Silybum marianum extract (Figure 2 (e)) indicate the melting point at 94.50 □, 147.78 □, and 125.42 □ respectively.

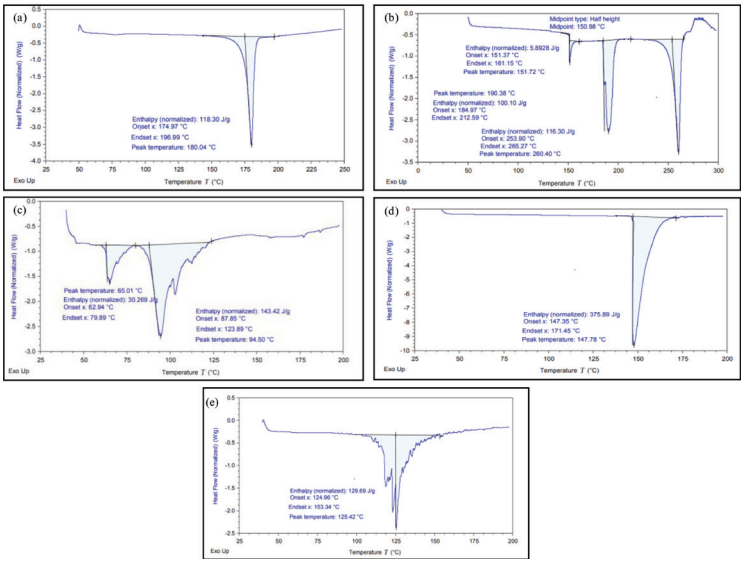

Figure 2: Differential scanning calorimetry (DSC) thermograms of (a) Curcumin showing an endothermic peak at 180.04 °C, (b) Hesperidin with an endothermic peak within the 258–262 °C range, (c) *Aegle marmelos* methanolic extract showing a melting point at 94.50 °C, (d) *Solanum nigrum* extract with a melting point at 147.78 °C, and (e) *Silybum marianum* extract showing a melting point at 125.42 °C.

- **Calibration curves**

When the samples were scanned at 400–200 nm, the peak wavelengths (Figure 3) were observed at 280 nm, 284 nm, 269 nm, 317 nm, and 275 nm for (a) curcumin, (b) hesperidin, (c) *Aegle marmelos* methanolic extract, (d) *Solanum nigrum* extract, and (e) *Silybum marianum* extract respectively.

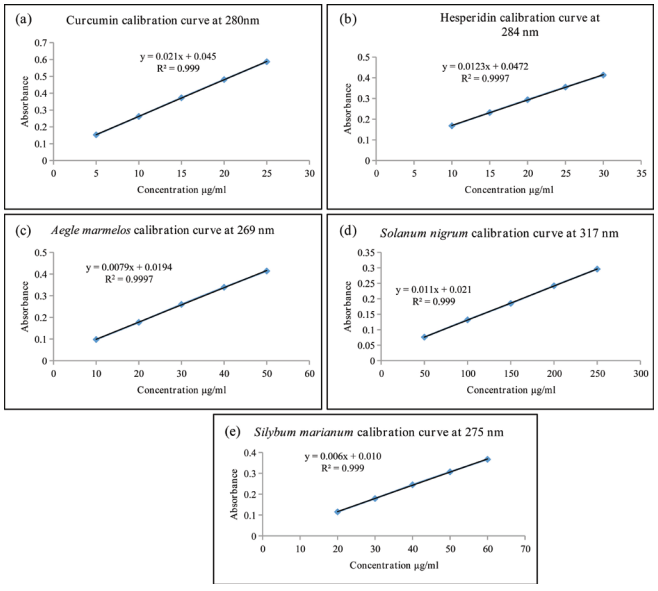

Figure 3: Calibration curves showing regression equations and R^2 values for (a) curcumin, (b) hesperidin, (c) *Aegle marmelos* methanolic extract, (d) *Solanum nigrum* extract, and (e) *Silybum marianum* extract.

3.3. Pre-compression Evaluations

The pre-compression evaluation of formulations F1–F13, including bulk density, tapped density, angle of repose, Carr's index, and Hausner ratio, is shown in Table 5. The tablets' pre-compression evaluation showed excellent and good flow properties, and all relevant parameters indicated compliance within specified limits. The developed formulations were found to have good bulk as well as tapped densities. Excellent and good flow properties have been shown by the angle of repose, which was found to be between 18.43 and 26.57, which is below 30 (Ravikkumar *et al.*, 2024). Carr's index is less than 16% and Hausner's ratio is less than 1.25, indicating good flow characteristics, which provide suitable processing of drugs (Ravikkumar *et al.*, 2024; Musuc *et al.*, 2021).

Table 5: Evaluation of Physical Properties of Powder Blend of All Formulations

Formulation	Bulk Density (gm/ml)	Tapped Density (gm/ml)	Angle of Repose (θ)	Carr's Index (%)	Hausner's Ratio
F1	0.465±0.01	0.541±0.05	20.14°±0.31	13.953±0.02	1.162±0.03
F2	0.357±0.04	0.417±0.02	23.5°±0.29	14.286±0.06	1.167±0.02
F3	0.377±0.03	0.435±0.04	19.44°±0.42	13.208±0.03	1.152±0.03
F4	0.392±0.03	0.444±0.02	26.57°±0.53	11.765±0.02	1.133±0.06
F5	0.364±0.06	0.417±0.02	19.8°±0.29	9.727±0.04	1.096±0.05
F6	0.385±0.02	0.444±0.04	19.8°±0.36	13.462±0.03	1.156±0.03
F7	0.377±0.04	0.444±0.03	18.43°±0.78	15.094±0.02	1.178±0.04
F8	0.345±0.07	0.392±0.06	23.75°±0.47	12.069±0.05	1.137±0.01
F9	0.377±0.03	0.426±0.02	19.98°±0.43	11.321±0.04	1.128±0.03
F10	0.408±0.05	0.455±0.04	24.3°±0.51	10.204±0.02	1.114±0.06
F11	0.385±0.01	0.426±0.08	19.79°±0.39	9.615±0.07	1.106±0.05
F12	0.385±0.02	0.444±0.01	19.44°±0.41	13.462±0.03	1.156±0.07
F13	0.364±0.04	0.435±0.02	20.37°±0.42	15.364±0.03	1.176±0.02

3.4. Post-compression Evaluations

A number of assessment tests, including dimension, hardness, friability, weight variation, and content consistency, were performed on the prepared tablets in accordance with standards. All of the tablets' dimensions were determined to be consistent, demonstrating the punching process' effectiveness (Table 6). After evaluation, it was found that all parameters for the polyherbal tablets that were produced utilizing the direct compression method met the specifications that were needed (Ravikkumar *et al.*, 2024; Musuc *et al.*, 2021; Zhao *et al.*, 2022). Friability is less than 1%, i.e., 0.29%–0.57%, and the weight variation is between 1.01% and 2.3%. All of the parameters, F1 to F13, are within acceptable limits, but Formulation F5 closely approximates the optimized formulation.

Table 6: Evaluation of Post-compression Parameters of Different Formulations

Formulation	% Weight Variation	Thickness (mm)	Diameter (mm)	Friability (%)	% Moisture Content
F1	1.55±0.3	4.0±0.02	8.8±0.11	0.43±0.01	3.901±0.4
F2	1.82±0.3	3.8±0.01	8.8±0.08	0.35±0.08	3.784±0.2
F3	1.62±0.2	3.9±0.03	8.7±0.01	0.40±0.10	3.832±0.3
F4	2.01±0.6	3.8±0.02	8.6±0.12	0.57±0.02	4.021±0.4
F5	1.32±0.2	3.9±0.01	8.8±0.09	0.37±0.08	3.579±0.3
F6	1.95±0.2	4.0±0.03	8.8±0.12	0.43±0.11	3.852±0.1
F7	1.66±0.3	3.9±0.02	8.7±0.09	0.40±0.04	3.852±0.3
F8	2.27±0.5	3.9±0.04	8.8±0.02	0.39±0.02	4.111±0.3
F9	1.62±0.3	4.0±0.03	8.8±0.04	0.41±0.04	3.863±0.2

F10	1.59±0.2	4.0±0.02	8.6±0.11	0.29±0.11	3.411±0.1
F11	1.39±0.4	3.8±0.01	8.7±0.01	0.41±0.04	3.289±0.3
F12	1.62±0.2	3.9±0.02	8.8±0.09	0.40±0.01	3.863±0.2
F13	1.98±0.1	3.9±0.04	8.8±0.12	0.37±0.11	3.706±0.3

3.5. Response Surface Methodology for Optimization of Tablet

A Central Composite Design (CCD), a response surface methodology, was used in experimental design to analyze the relationship between independent variables and a response (dependent) variable. To examine the relationship between the independent variables Hardness and Disintegration Time and the dependent variables MCC and Starch, the current study used a quadratic model (Table 7).

Table 7: Results of Experimental Variables

Formulation Batches	MCC (X1)	Starch (X2)	Hardness (Kg/cm2)	Disintegration Time (sec)
F1	50	40	5.8	114
F2	55	27.9289	3.2	82
F3	55	35	5.1	93
F4	50	30	3.5	92
F5	60	30	4.7	77
F6	55	35	5.0	92
F7	55	35	5.1	93
F8	47.9289	35	4.8	107
F9	55	35	5.2	93
F10	62.0711	35	5.7	82
F11	60	40	6.5	91
F12	55	35	5.1	93
F13	55	42.0711	6.2	106

3.6. Effect of Independent Variables on Hardness of the Tablet

Experimental results were analyzed using ANOVA, and tablet hardness was evaluated based on the p-values of the regression coefficients. Insufficient hardness can cause tablets to break easily, whereas adequate hardness improves mechanical strength and overall stability. Therefore, optimal concentrations of the formulation components were identified to ensure the required hardness and to enhance resistance to breakage.

The influence of the independent variables on the response was assessed using a statistical model incorporating linear, quadratic, interaction, and polynomial terms. A factor was considered to have a significant effect on the response variable R1 if the p-value was less than 0.05 ($p < 0.05$). Non-significant factors ($p > 0.05$) were removed to simplify the regression model.

According to Table 7, tablet hardness ranged from 3.2 to 6.5 kg/cm². The quadratic model demonstrated a good fit for hardness, supported by a highly significant F-value (123.92) and p-value (< 0.0001). The lack-of-fit p-value was 6.45 ($p > 0.05$), indicating a non-significant lack of fit relative to pure error and confirming the suitability of the model. The model accuracy was further verified through ANOVA, producing an R^2 value of 0.9888, indicating strong correlation between predicted and observed values.

The software-generated quadratic equation for hardness (R1) is:

$$\boldsymbol{R1}(\boldsymbol{Hardness}) = 5.1 + 0.397A + 1.043B - 0.125AB + 0.113A^2 - 0.163B^2$$

The equation indicates that both factor A (MCC) and factor B (starch) exert a positive effect on hardness. Figures 4(a) and 4(b) illustrate the contour and 3D surface plots, showing that hardness increases with increasing MCC concentration. Similarly, increasing starch concentration also enhances hardness, which may be attributed to the long-chain polymeric nature of both starch and MCC (Liew *et al.*, 2021; Zhao *et al.*, 2022). Starch acts as a binder and swells in the presence of water, leading to chain extension and entanglement with MCC polymers (Liew *et al.*, 2021). These findings align with previously reported studies (Liew *et al.*, 2021; Loke *et al.*, 2024). The negative coefficient of B^2 indicates a diminishing effect on hardness at higher starch concentrations. The effects of AB and A^2 were excluded from final interpretation due to p-values > 0.05.

3.7. Effect of Independent Variables on Disintegration Time of the Tablet

The disintegration time (DT) of the formulations ranged from 77 to 114 seconds (Table 9). The quadratic model was found to be highly suitable for DT, supported by a significant F-value (548.33) and p-value (< 0.0001). The lack-of-fit p-value of 4.22 ($p > 0.05$) indicated a non-significant lack of fit, confirming that the model was appropriate. ANOVA further validated the model's accuracy, yielding a high R^2 value of 0.9975, indicating a strong correlation between predicted and observed values.

The quadratic equation for DT (R2) is:

$$\boldsymbol{R2}(\boldsymbol{DT}) = 92.80 - 9.17A + 8.74B - 2.00AB + 0.6625A^2 + 0.4125B^2$$

The equation shows that factor B (starch) positively influences disintegration time, increasing DT, whereas factor A (MCC) has a negative effect, reducing DT. Figures 4(c) and 4(d) demonstrate through contour and 3D surface plots that increasing MCC concentration leads to decreased disintegration time, consistent with previous reports (Zhao *et al.*, 2022). In contrast, higher starch concentrations increase DT, likely due to the swelling nature of starch (Liew *et al.*, 2021).

The interaction term AB suggests that the combined effect of MCC and starch contributes to a reduction in disintegration time. The quadratic term B^2 was excluded from interpretation due to its p-value being greater than 0.05.

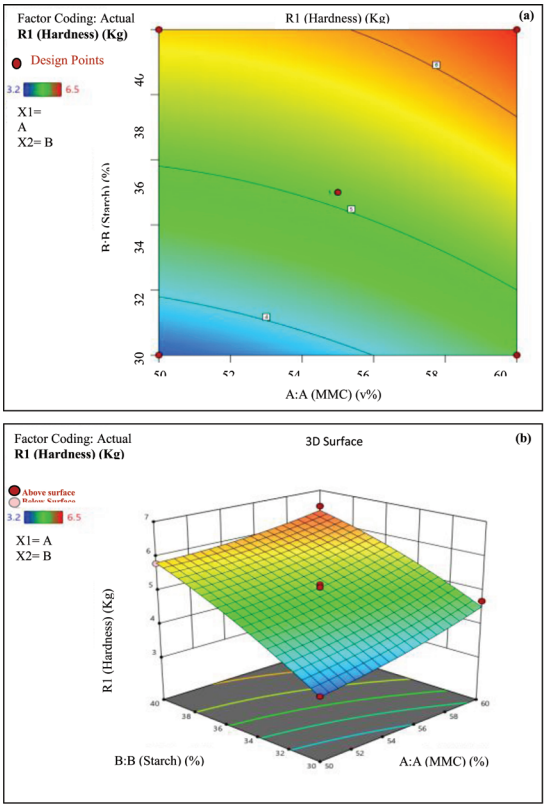

Figure 4. Contour plots and 3D response surface plots showing the effect of MCC (X_1) and starch (X_2) on tablet hardness in (a) and (b), and on disintegration time in (c) and (d), respectively.

3.6. Optimization

Disintegration time and hardness data for all formulations were used to identify the optimized batch. The Design-Expert 13 software recommended the optimal formulation by predicting the most favorable levels of the independent variables. The optimal concentrations were determined to be 59.186% MCC and 31.781% starch. For this optimized polyherbal tablet, the expected responses were a hardness of 4.8 kg/cm² and a disintegration time of 81.2 seconds.

- **Composition of the Optimized Tablet Batch**

A major outcome of this study was the development of the optimized polyherbal tablet formulation (Figure 5). The formulation incorporates multiple herbal constituents, each selected for their therapeutic properties. Table 8 presents the finalized optimized formulation (F14).

Table 8: Optimized Polyherbal Formulation (F14)

Ingredients	**Quantity (mg)**
MCC	59.186
Starch	31.781
Polyvinyl pyrrolidone K30	6
Sodium bicarbonate	3
Magnesium stearate	1
Hesperidin	30
Curcumin	30
Aegle marmelos leaves extract	30
Solanum nigrum leaves extract	30
Silybum marianum seed extract	30

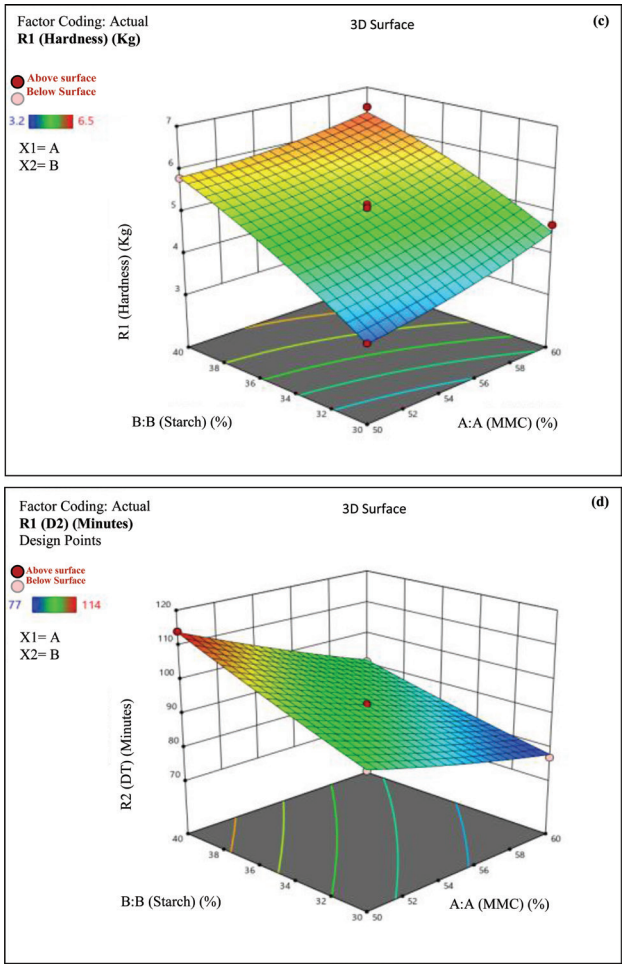

Figure 5: Optimized Polyherbal Tablets (F14)

- **Evaluation of Optimized Batch of Tablet**

A batch of optimized tablets was evaluated for weight variation, drug content, moisture content, thickness, diameter, friability, and percentage cumulative drug release as shown in Table 9. In-vitro dissolution studies were carried out to determine how the drugs are released from the tablets under simulated physiological conditions. The percentages of drug release of the optimized polyherbal formulation for curcumin, hesperidin, *Aegle marmelos*, *Solanum nigrum*, and *Silybum marianum* were determined to be 71.57%, 74.25%, 90.86%, 94.91%, and 91.50%, respectively.

Table 9: Result of the Evaluated Parameters for Optimized Formulation (F14)

Parameters	Results
% Weight variation (Limit ± 5%)	1.44±0.2
Thickness (mm)	3.8±0.01
Diameter (mm)	8.8±0.03
Friability (%)	0.41±0.01
% Moisture Content	3.9±0.4
Hardness (Kg/cm²)	4.9±0.08
Disintegration Time (sec)	82.6±0.11
Drug Content (%)	Curcumin: 82.29%; Hesperidin: 89.50%; *Aegle marmelos*: 93.86%; *Solanum nigrum*: 98.12%; *Silybum marianum*: 96.23%
Cumulative drug release (%)	Curcumin: 71.57%; Hesperidin: 74.25%; *Aegle marmelos*: 90.86%; *Solanum nigrum*: 94.91%; *Silybum marianum*: 91.50%

- **Drug Release Kinetics**

In order to observe the drug release mechanism, the in-vitro dissolution profile of the optimized polyherbal tablet formulation (F14) was further examined using linear regression in accordance with zero-order, first-order, Higuchi, Korsmeyer–Peppas, and Hixson–Crowell models, as well as the goodness-of-fit test. Table 10 displays the findings of the analysis. The Hixson–Crowell model and the formulation of the polyherbal tablet under investigation exhibited a satisfactory connection. The formulation follows a non-fickian super case II release mechanism, as indicated by the Korsmeyer–Peppas plot, where *n* is more than 1 (Ekenna *et al.*, 2022; Venkatesh *et al.*, 2022).

Table 10: R^2 Values for Optimized Formulations for Different Mathematical Models

Phytochemical/ Extract	Regression Coefficient (R^2)	'n' value
	Zero-order	1st Order
Curcumin	0.98	0.978
Hesperidin	0.982	0.958
Aegle marmelos	0.997	0.911
Solanum nigrum	0.990	0.919
Silybum marianum	0.982	0.881

The formulation of the polyherbal tablet under study shows an acceptable correlation with the Hixson–Crowell model, as evidenced by the highest R^2 values obtained as given in Table 12. According to the Korsmeyer–Peppas plot, the value of the exponent (*n*) is greater than 1, which indicates that the formulation follows a non-fickian super case II release mechanism, as shown in Table 10.

4. Conclusion

In this research study, polyherbal tablet was formulated and evaluated, comprising curcumin, hesperidin, and extracts from *Aegle marmelos*, *Solanum nigrum*, and *Silybum marianum* for the management of liver cirrhosis and hepatoprotective action. The choice of phytochemicals was based on literature findings. From our study, it was found that the optimized tablets showed good properties, including thickness, disintegration time, hardness, friability, and weight variation, and fell within a predetermined range. The formulation of the polyherbal tablet correlates with the Hixson-Crowell model, indicating a satisfactory agreement between the theoretical and experimental dissolving profiles. A non-Fickian super case II release mechanism was indicated by an 'n' value greater than 1, underscoring the intricacy of drug release from these tablets. Additional research, including in vivo investigations and clinical trials, may validate its therapeutic efficacy and safety, potentially offering a useful alternative treatment for liver-related conditions.

Abbreviations

HSP: Hesperidin; **PVP**: Polyvinylpyrrolidone; **FTIR**: Fourier Transform Infrared Spectroscopy; **APIs**: Active Pharmaceutical Agents; **KBr**: Potassium Bromide; **DSC**: Differential Scanning Calorimetry; **HR**: Hausner's Ratio; **MCC**: Microcrystalline Cellulose; **CCD**: Central Composite Design.

Acknowledgement

The authors gratefully acknowledge the support and facilities provided by Guru Gobind Singh College of Pharmacy, Yamunanagar, Haryana.

Authorship Contribution

Kamaljeet: Conducted research. Rameshwar Das: Provided supervision and validated the results. Priyanka Kriplani: Designed the study. Prabhjot Kaur: Conducted the research and prepared the original draft.

Funding

This research did not receive any specific grant from funding agencies in the public, commercial, or not-for-profit sectors.

Ethical Approval

Ethical approval was not required for this study.

Declaration

This is an original article and has neither been submitted elsewhere nor published previously.

Conflict of Interest

The authors declare that there is no conflict of interest.

References

Aghazadeh, S., Amini, R., Yazdanparast, R., & Ghaffari, S. H. (2011). Anti-apoptotic and anti-inflammatory effects of Silybum marianum in treatment of experimental steatohepatitis. *Experimental and toxicologic pathology*, *63*(6), 569-574.

Ahmad, W., Amir, M., Ahmad, A., Ali, A., Ali, A., Wahab, S., Barkat, H.A., Ansari, M.A., Sarafroz, M., Ahmad, A. & Alam, P. (2021). Aegle marmelos leaf extract phytochemical analysis, cytotoxicity, in vitro antioxidant and antidiabetic activities. *Plants*, *10*(12), 2573.

Bhardwaj, R. L., & Nandal, U. (2015). Nutritional and therapeutic potential of bael (Aegle marmelos Corr.) fruit juice: a review. *Nutrition* & *Food Science*, *45*(6), 895-919.

Chimagave, S. S., Jalalpure, S. S., Patil, A. K., & Kurangi, B. K. (2022). Development and validation of stability indicating UV-spectrophotometric method for the estimation of hesperidin in bulk drugs, plant extract, Ayurveda formulation and nanoformulation. *Indian J Pharm Educ Res*, *56*(3), 865-872.

Cofano, M., Saponara, I., De Nunzio, V., Pinto, G., Aloisio Caruso, E., Centonze, M., & Notarnicola, M. (2025). Hesperidin Is a Promising Nutraceutical Compound in Counteracting the Progression of NAFLD In Vitro. *International Journal of Molecular Sciences*, *26*(13), 5982.

Devarbhavi, H., Asrani, S. K., Arab, J. P., Nartey, Y. A., Pose, E., & Kamath, P. S. (2023). Global burden of liver disease: 2023 update. *Journal of hepatology*, *79*(2), 516-537.

Ekenna, I. C., & Abali, S. O. (2022). Comparison of the use of kinetic model plots and DD solver software to evaluate the drug release from griseofulvin tablets. *Jornal of Drug Delivery Ther*, *12*(2-S), 5-13.

Federico, A., Dallio, M., & Loguercio, C. (2017). Silymarin/silybin and chronic liver disease: a marriage of many years. *Molecules*, *22*(2), 191.

Gupta, A., Thomas, T., & Khan, S. (2018). Physicochemical, phytochemical screening and antimicrobial activity of Aegle marmelos. *Pharmaceutical and Biosciences Journal*, 17-24.

Jiang, G., Sun, C., Wang, X., Mei, J., Li, C., Zhan, H., Liao, Y., Zhu, Y. & Mao, J. (2022). Hepatoprotective mechanism of Silybum marianum on nonalcoholic fatty liver disease based on network pharmacology and experimental verification. *Bioengineered*, *13*(3), 5216-5235.

Khonche, A., Huseini, H. F., Gholamian, M., Mohtashami, R., Nabati, F., & Kianbakht, S. (2019). Standardized Nigella sativa seed oil ameliorates hepatic steatosis, aminotransferase and lipid levels in non-alcoholic fatty liver disease: A randomized, double-blind and placebo-controlled clinical trial. *Journal of Ethnopharmacology*, *234*, 106-111.

Kornerup, L. S., Kraglund, F., Askgaard, G., Vilstrup, H., & Jepsen, P. (2025). Cirrhosis epidemiology in Denmark 1998–2022, and 2030 forecast. *JHEP Reports*, *7*(5).

Li, X., Yao, Y., Wang, Y., Hua, L., Wu, M., Chen, F., Deng, Z.Y.& Luo, T. (2022). Effect of hesperidin supplementation on liver metabolomics and gut microbiota in a high-fat diet-induced NAFLD mice model. *Journal of Agricultural and Food Chemistry*, *70*(36), 11224-11235.

Liew, K. B., & Peh, K. K. (2021). Investigation on the effect of polymer and starch on the tablet properties of lyophilized orally disintegrating tablet. *Archives of pharmacal research*, *44*(8), 1-10.

Loke, Y.H., Phang, H.C., Gobal, G., Vijayaraj Kumar, P., Kee, P.E., Widodo, R.T., Goh, B.H.& Liew, K. B. (2024). Application of cocoa butter for formulation of fast melt tablets containing memantine hydrochloride. *Drug Development and Industrial Pharmacy*, *50*(10), 845-855.

Lukic, I., Milovanovic, S., Pantic, M., Srbljak, I., Djuric, A., Tadic, V., & Tyśkiewicz, K. (2022). Separation of

high-value extracts from Silybum marianum seeds: Influence of extraction technique and storage on composition and bioactivity. *Lwt*, *160*.

Majumder, K. K., Sharma, J. B., Kumar, M., Bhatt, S., & Saini, V. (2020). Development and validation of UV-Visible spectrophotometric method for the estimation of curcumin in bulk and pharmaceutical formulation. *Pharmacophore*, *11*(1-2020), 115-121.

Mancak, M., Altintas, D., Balaban, Y., & Caliskan, U. K. (2024). Evidence-based herbal treatments in liver diseases. In *Hepatology forum,* 5(1), 50.

Mirhafez, S.R., Azimi-Nezhad, M., Dehabeh, M., Hariri, M., Naderan, R.D., Movahedi, A., Abdalla, M., Sathyapalan, T. & Sahebkar, A. (2021). The effect of curcumin phytosome on the treatment of patients with non-alcoholic fatty liver disease: a double-blind, randomized, placebo-controlled trial. In *Pharmacological properties of plant-derived natural products and implications for human health,* 25-35.

Morshedzadeh, N., Ramezani Ahmadi, A., Behrouz, V., & Mir, E. (2023). A narrative review on the role of hesperidin on metabolic parameters, liver enzymes, and inflammatory markers in nonalcoholic fatty liver disease. *Food Science & Nutrition*, *11*(12), 7523-7533.

Morteza-Semnani, K., Saeedi, M., Akbari, J., Hedayati, S., Hashemi, S.M.H., Rahimnia, S.M., Babaei, A., Ghazanfari, M., Haghani, I. & Hedayati, M. T. (2022). Green formulation, characterization, antifungal and biological safety evaluation of terbinafine HCl niosomes and niosomal gels manufactured by eco-friendly green method. *Journal of Biomaterials Science, Polymer Edition*, *33*(18), 2325-2352.

Mukhtar, S., Xiaoxiong, Z., Khalid, W., Moreno, A., & Lorenzo, J. M. (2023). In vitro antioxidant capacity of purified bioactive compounds in Milk thistle seed (Silybum marianum) along with phenolic profile. *Food Analytical Methods*, *16*(4), 651-663.

Musuc, A.M., Anuta, V., Atkinson, I., Sarbu, I., Popa, V.T., Munteanu, C., Mircioiu, C., Ozon, E.A., Nitulescu, G.M. & Mitu, M. A. (2021). Formulation of chewable tablets containing carbamazepine-β-cyclodextrin inclusion complex and f-melt disintegration excipient. The mathematical modeling of the release kinetics of carbamazepine. *Pharmaceutics*, *13*(6), 915.

Narukulla, S., Bogadi, S., Tallapaneni, V., Sanapalli, B.K.R., Sanju, S., Khan, A.A., Malik, A., Barai, H.R., Mondal, T.K., Karri, V.V.S.R. & Papadakis, M. (2024). Comparative study between the Full Factorial, Box–Behnken, and Central Composite Designs in the optimization of metronidazole immediate release tablet. *Microchemical Journal*, *207*.

Ngu, M. H., Norhayati, M. N., Rosnani, Z., & Zulkifli, M. M. (2022). Curcumin as adjuvant treatment in patients with non-alcoholic fatty liver (NAFLD) disease: A systematic review and meta-analysis. *Complementary Therapies in Medicine*, *68*.

Panchal, P. M., & Shah, D. A. (2025). Simultaneous quantification of quercetin and solasodine biomarkers from Solanum nigrum Linn. berry extract using a validated high-performance thin-layer chromatography−densitometric method. *JPC–Journal of Planar Chromatography–Modern TLC*, 1-11.

Park, M.N., Rahman, M.A., Rahman, M.H., Kim, J.W., Choi, M., Kim, J.W., Choi, J., Moon, M., Ahmed, K.R.& Kim, B. (2022). Potential therapeutic implication of herbal medicine in mitochondria-mediated oxidative stress-related liver diseases. *Antioxidants*, *11*(10), 2041.

Ravikkumar, V.R., Patel, B.D., Rathi, S., Parthiban, S., Upadhye, M.C., Shah, A.M., Rehan, S.S.A., Samanta, S. & Singh, S. (2024). Formulation and evaluation of Drumstick leaves tablet as an immunomodulator. *Zhongguo Ying Yong Sheng Li Xue Za Zhi*, *40*.

Robinson, K., Mock, C., & Liang, D. (2015). Pre-formulation studies of resveratrol. *Drug development and industrial pharmacy*, *41*(9), 1464-1469.

Różański, G., Kujawski, S., Newton, J. L., Zalewski, P., & Słomko, J. (2021). Curcumin and biochemical parameters in metabolic-associated fatty liver disease (MAFLD)—A review. *Nutrients*, *13*(8), 2654.

Shahrebabak, M. G., Haghighi, S. P. S., Ravankhah, M., Zare, A., Bazyari, V., & Izadi, B. (2025). A Systematic Review and Meta-analysis of Randomised Controlled Trials on Curcumin-Piperine Supplementation: A Promising Strategy for Managing Lipid Profiles and Liver Health in Non-alcoholic Fatty Liver Disease. *Journal of Herbal Medicine*, *51*.

Shaker, E., Mahmoud, H., & Mnaa, S. (2010). Silymarin, the antioxidant component and Silybum marianum extracts prevent liver damage. *Food and Chemical Toxicology*, *48*(3), 803-806.

Sharma, R., Bansal, M., Garg, A., Agarwal, V., & Sharma, D. (2023). Formulation and Evaluation of Sustain Release Matrix Tablet of Aceclofenac. *International Journal of Health Advancement and Clinical Research (tz)*, *1*(1).

Singanan, V., Singanan, M., & Begum, H. (2007). The hepatoprotective effect of bael leaves (Aegle marmelos) in alcohol induced liver injury in albino rats. *International Journal of Science & Technology*, *2*(2), 83-92.

Sivaslioglu, A., & Goktas, Z. (2024). A comprehensive review on the impact of hesperidin and its aglycone hesperetin on metabolic dysfunction-associated steatotic liver

disease and other liver disorders. *Nutrition research reviews*, 1-37.

Solati, Z., Baharin, B. S., & Bagheri, H. (2014). Antioxidant property, thymoquinone content and chemical characteristics of different extracts from Nigella sativa L. seeds. *Journal of the American Oil Chemists' Society*, *91*(2), 295-300.

Tafere, C., Yilma, Z., Abrha, S., & Yehualaw, A. (2021). Formulation, in vitro characterization and optimization of taste-masked orally disintegrating co-trimoxazole tablet by direct compression. *PloS one*, *16*(3).

Tang, G., Zhang, L., Tao, J., & Wei, Z. (2021). Effect of Nigella sativa in the treatment of nonalcoholic fatty liver disease: A systematic review and meta-analysis of randomized controlled trials. *Phytotherapy Research*, *35*(8), 4183-4193.

Terrault, N. A., Francoz, C., Berenguer, M., Charlton, M., & Heimbach, J. (2023). Liver transplantation 2023: status report, current and future challenges. *Clinical Gastroenterology and Hepatology*, *21*(8), 2150-2166.

Tiwari, A., Surendra, G., Meka, S., Varghese, B., Vishwakarma, G., & Adela, R. (2022). The effect of Nigella sativa on non-alcoholic fatty liver disease: A systematic review and meta-analysis. *Human Nutrition & Metabolism*, *28*, 200146.

Venkatesh, D.N., Meyyanathan, S.N., Kovacevic, A., Zielińska, A., Fonseca, J., Eder, P., Dobrowolska, A. & Souto, E. B. (2022). Effect of hydrophilic polymers on the release rate and pharmacokinetics of acyclovir tablets obtained by wet granulation: in vitro and in vivo assays. *Molecules*, *27*(19).

Vlizlo, V., Prystupa, O., Slivinska, L., Gutyj, B., Maksymovych, I., Shcherbatyy, A., Lychuk, M., Partyka, U., Chernushkin, B., Rusyn, V. & Leskiv, K. (2023). Treatment of animals with fatty liver disease using a drug based on the seeds of Silybum marianum. *Regulatory Mechanisms in Biosystems*, *14*(3), 424-431.

Yari, Z., Cheraghpour, M., Alavian, S. M., Hedayati, M., Eini-Zinab, H., & Hekmatdoost, A. (2021). The efficacy of flaxseed and hesperidin on non-alcoholic fatty liver disease: an open-labeled randomized controlled trial. *European journal of clinical nutrition*, *75*(1), 99-111.

Zhang, C., Shao, H., Han, Z., Liu, B., Feng, J., Zhang, J., Zhang, W., Zhang, K., Yang, Q. & Wu, S. (2023). Development and in vitro–in vivo correlation evaluation of IMM-H014 extended-release tablets for the treatment of fatty liver disease. *International Journal of Molecular Sciences*, *24*(15), 12328.

Zhao, H., Shi, C., Zhao, L., Wang, Y., & Shen, L. (2022). Influences of different microcrystalline cellulose (MCC) grades on tablet quality and compression behavior of MCC-lactose binary mixtures. *Journal of Drug Delivery Science and Technology*, *77*.